

Contribution of Functional Groups to the Raman Spectrum of Nanodiamond Powders

Vadym Mochalin, Sebastian Osswald, and Yury Gogotsi*

A. J. Drexel Nanotechnology Institute and Department of Materials Science and Engineering,
Drexel University, 3141 Chestnut Street, Philadelphia, Pennsylvania 19104

Received July 28, 2008. Revised Manuscript Received November 4, 2008

In depth understanding of Raman spectra of carbon nanomaterials led to the extension of this technique from simple carbon allotrope detection (fingerprinting) to analysis of the dimensions and ordering of graphene, graphite and nanotubes. In characterization of nanodiamond powders, which have been attracting attention as one of the most promising carbon nanomaterials, Raman spectroscopy is still mainly used only for detecting the diamond phase because of poor understanding of other spectral features. In this paper, we critically examine different explanations of the broad asymmetric Raman band between 1500 and 1800 cm^{-1} present in all nanodiamond powders and provide an assignment of the contributing peaks, solving one of the major remaining mysteries in Raman spectroscopy of nanodiamond. By using nanodiamond powders with different and well-controlled surface chemistries, as well as in situ Raman measurements at elevated temperatures, we show that these peaks originate from O–H bending vibrations either from the surface functional groups or adsorbed water with contributions (shoulders) coming from sp^2 carbon and C=O stretching vibrations. The observation of a strong O–H contribution to the Raman spectrum of nanodiamond raises concerns regarding the use of water as a coolant during the Raman spectra acquisition, because water may affect Raman spectra in the wavenumber ranges corresponding to bending and stretching O–H vibrations.

Introduction

Nanodiamond produced by detonation synthesis (ND) has attracted much attention over the past decade.^{1–5} Studies of this novel nanomaterial aim to understand and tailor its unique properties rooted in the combination of an inert diamond core with a surface rich in functional groups.⁶ First discovered in the 1960s in the former Soviet Union, ND is one of few nanomaterials produced on a commercial scale. A simple production process, which uses expired munitions as energy and a carbon source for the detonation synthesis, results in a moderate price; this leads to numerous applications of ND in composites,⁷ lubricants, polishing compositions,⁵ heat spreaders, and sorbents.⁸ New advanced applications, especially in medicine,⁹ require a better understanding of the ND structure, phase composition, and surface chemistry. ND powders are composed of aggregates of primary

particles with an average size of 5 nm, comprising a diamond core partially or completely covered by layers of graphitic and/or amorphous carbon, and bearing carboxyl-, hydroxyl-, carbonyl-, nitrogen-, and sulfur-containing functionalities on the surface.⁶

Raman and IR spectroscopy, being complementary techniques, provide valuable insights into phase composition and surface terminations of nanomaterials. An in-depth understanding of the spectral features of carbon nanomaterials allowed the use of Raman spectroscopy to extend beyond carbon allotrope identification to a stage where it is currently used to determine diameter and size distribution of SWCNTs,¹⁰ number of graphene layers,¹¹ graphitization degree, and the in-plane size of graphitic crystallites.¹² In the case of ND, however, there is an ongoing effort to better understand and assign all peak features in Raman spectra,^{13–21} and the use of Raman spectroscopy for analysis of ND is

* Corresponding author. E-mail: gogotsi@drexel.edu.

- (1) Shenderova, O. A.; Gruen, D. M. *Ultrananocrystalline Diamond: Synthesis, Properties, and Applications*; William Andrew: Norwich, NY, 2006; p 600.
- (2) Shenderova, O. A.; McGuire, G. Nanocrystalline Diamond. In *Nanomaterials Handbook*; Gogotsi, Y., Ed.; CRC Taylor and Francis Group: Boca Raton, FL, 2006; pp 203–237.
- (3) Shenderova, O. A.; Zhirnov, V. V.; Brenner, D. W. Carbon nanostructures. *Crit. Rev. Solid State Mater. Sci.* **2002**, 27 (3–4), 227–356.
- (4) Gruen, D. M.; Shenderova, O. A.; Vul, A. Y., *Synthesis, Properties and Applications of Ultrananocrystalline Diamond*; Springer: Dordrecht, The Netherlands, 2005; Vol. 192, p 401.
- (5) Dolmatov, V. Y. *Usp. Khim.* **2007**, 76 (4), 375–397.
- (6) Osswald, S.; Yushin, G.; Mochalin, V.; Kucheyev, S. O.; Gogotsi, Y. *J. Am. Chem. Soc.* **2006**, 128 (35), 11635–11642.
- (7) Shenderova, O.; Tyler, T.; Cunningham, G.; Ray, M.; Walsh, J.; Casulli, M.; Hens, S.; McGuire, G.; Kuznetsov, V.; Lipa, S. *Diamond Relat. Mater.* **2007**, 16 (4–7), 1213–1217.

- (8) Gibson, N.; Fitzgerald, Z.; Luo, T.-J.; Shenderova, O.; Grichko, V.; Bondar, V.; Puzyr, A.; Brenner, D. W. Nanodiamonds for Detoxification. In *Nanotech 2007*; Santa Clara, CA, May 20–24, 2007; Laudon, M.; Romanowicz, B., Eds.; Nano Science and Technology Institute: Cambridge, MA, 2007; pp 713–716.
- (9) Mitura, S.; Niedzielski, P.; Walkowiak, B. *Nanodiamond New Technologies for Medical Applications: Studying and Production of Carbon Surfaces Allowing for Controllable Bioactivity*; Wydawnictwo Naukowe PWN: Warsaw, Poland, 2006; p 287.
- (10) Rao, A. M.; Richter, E.; Bandow, S.; Chase, B.; Eklund, P. C.; Williams, K. A.; Fang, S.; Subbaswamy, K. R.; Menon, M.; Thess, A.; Smalley, R. E.; Dresselhaus, G.; Dresselhaus, M. S. *Science* **1997**, 275 (5297), 187–191.
- (11) Ferrari, A. C. *Solid State Commun.* **2007**, 143 (1–2), 47–57.
- (12) Tuinstra, F.; Koenig, J. L. *J. Chem. Phys.* **1970**, 53 (3), 1126–1130.
- (13) Birrell, J.; Gerbi, J. E.; Auciello, O.; Gibson, J. M.; Johnson, J.; Carlisle, J. A. *Diamond Relat. Mater.* **2005**, 14 (1), 86–92.
- (14) Ferrari, A. C.; Robertson, J. *Phys. Rev. B* **2001**, 63, 12.

still limited to simple identification of the diamond phase. One of the main reasons is a poor understanding of nondiamond features in Raman spectra of ND. For example, only recently, after 12 years of confusion, the 1150 cm^{-1} peak was correctly assigned to *trans*-polyacetylene fragments instead of nanocrystalline or amorphous diamond.¹⁴

With tremendous progress in computational techniques and an increase in computer power, first principles predictions of Raman spectra recently became possible for ND particles up to 1 nm size.²² However, the correct prediction of a Raman spectrum of a complex 5 nm ND particle is not possible, therefore experimental spectroscopy studies are still required. Because the Raman peak of ND is very weak, it is completely covered by the D-band of graphitic carbon in visible Raman spectra. Thus, the use of UV lasers is required.

The UV Raman spectrum of ND consists of several characteristic features:^{13,15,17,20,21} the first-order Raman mode of the cubic diamond lattice which is broadened and red-shifted in ND (a peak at $\sim 1325\text{ cm}^{-1}$) compared to bulk diamond (1332 cm^{-1}); a double-resonant D-band around 1400 cm^{-1} (at 325 nm excitation), resulting from disordered and amorphous sp^2 carbon; and a broad asymmetric peak between 1500 and 1800 cm^{-1} . The latter peak has at least four different explanations proposed for its origin. Most often it is labeled as the “G-band” and assigned to the in-plane vibrations of graphitic carbon.^{13–15} However, this peak significantly differs from the G-band of graphitic materials both in shape and position.^{23,24} Therefore it is sometimes assigned to a mixed sp^2/sp^3 carbon structure,²⁵ or is referred to as a peak of “ sp^2 carbon”²⁶ or “ sp^2 clusters”²¹ without any explanation regarding the structure (amorphous, graphitic, etc.). Finally, there have been attempts to relate this peak to localized interstitial C=C pairs within the diamond lattice also known as “dumb-bell defects”.^{19,20} However, with plenty of various functional groups exposed on the ND surface, the broad band(s) between 1500 and 1800 cm^{-1} may result from overlapping Raman signals of sp^2 carbon species, surface groups such as OH, COOH, and C=C pairs embedded inside the diamond core. In this case, the peak position, intensity, width, and shape may all be influenced by the

interplay of these contributions, i.e., may be different for different types of ND. Taking into account the rich surface chemistry of ND, the lack of systematic studies on the contribution of functional groups into the Raman spectrum of ND is surprising.

Another major problem in Raman spectroscopy of ND is related to the laser radiation commonly used as an excitation source. Because of the small Raman cross-section of diamond in the visible light and the shielding effect of graphitic and amorphous carbon around the diamond core, UV lasers with excitation energy close to the bandgap of diamond (5.5 eV) are needed to amplify the Raman signal of ND. Although delivering more energy per quantum, the UV lasers heat up samples much more strongly than visible ones, and may lead to thermal damage and changes in sample composition. Several techniques have been proposed for cooling samples during Raman measurements, including continuous sample movement,^{27,28} minimization of the incident laser power,²⁸ incorporation into a KBr pellet,²⁷ use of cylindrical optics or shutters,²⁷ and the submerging of samples under water.^{20,29} Although water cooling seems to be the easiest way to avoid thermal damage, care should be taken when interpreting Raman results. H_2O vibrational modes (O–H bending at $\sim 1640\text{ cm}^{-1}$ and stretching at $3300\text{--}3500\text{ cm}^{-1}$) may potentially interfere with the weak Raman signal of ND. To the best of our knowledge, this interference has not yet been analyzed in literature and is traditionally underestimated in Raman measurements.

In this paper, we report Raman and FTIR spectra of ND powders with different diamond/nondiamond carbon ratios and surface chemistry, acquired under various conditions. In situ studies were used to analyze the temperature dependence of the 1640 cm^{-1} Raman peak in order to understand its origin. Contributions from surface functional groups and nondiamond carbon phases to the Raman spectrum of ND between 1500 and 1800 cm^{-1} will be discussed.

Experimental Section

ND powders UD50 and UD90 were supplied by NanoBlox, Inc. (USA). NDAlit powder was supplied by Alit (Ukraine). UD50 is the raw detonation soot with a content of nondiamond carbon $\sim 70\text{ wt } \%$ and a low content of surface functional groups.⁶ According to specifications provided by the manufacturer, UD90 contains 82% C, 0.79% H, and 2.5% N. Main ash impurities in UD90 are Ca (0.72%), Fe (0.68%), Mg (0.10%), and Pb (0.06%). UD90⁶ and NDAlit²⁹ are acid-purified powders with a nondiamond carbon content less than 30 wt % and numerous surface functional groups, which produce intense C=O, O–H, and weaker C–H peaks in IR spectra. As-received UD90 was modified using various procedures and resulting samples have been named accordingly: UD90Ox (air oxidized), UD90OxHCl (air oxidized, HCl treated) and UD90H (hydrogenated). UD90Ox was produced from UD90 by air oxidation at $425\text{ }^\circ\text{C}$ for 5 h.⁶ It has a diamond phase content of $\sim 95\text{ wt } \%$

- (15) Ferrari, A. C.; Robertson, J. *Philos. Trans. R. Soc. London, Ser. A* **2004**, 362 (1824), 2477–2512.
- (16) Lipp, M. J.; Baonza, V. G.; Evans, W. J.; Lorenzana, H. E. *Phys. Rev. B* **1997**, 56 (10), 5978–5984.
- (17) Nistor, L. C.; VanLanduyt, J.; Ralchenko, V. G.; Obraztsova, E. D.; Smolin, A. A. *Diamond Relat. Mater.* **1997**, 6 (1), 159–168.
- (18) Perevedentseva, E.; Karmenyan, A.; Chung, P. H.; Cheng, C. L. *J. Vac. Sci. Technol., B* **2005**, 23 (5), 1980–1983.
- (19) Praver, S.; Nemanich, R. J. *Philos. Trans. R. Soc. London, Ser. A* **2004**, 362 (1824), 2537–2565.
- (20) Praver, S.; Nugent, K. W.; Jamieson, D. N.; Orwa, J. O.; Bursill, L. A.; Peng, J. L. *Chem. Phys. Lett.* **2000**, 332 (1–2), 93–97.
- (21) Yoshikawa, M.; Mori, Y.; Obata, H.; Maegawa, M.; Katagiri, G.; Ishida, H.; Ishitani, A. *Appl. Phys. Lett.* **1995**, 67 (5), 694–696.
- (22) Filik, J.; Harvey, J. N.; Allan, N. L.; May, P. W.; Dahl, J. E. P.; Liu, S.; Carlson, R. M. K. *Phys. Rev. B* **2006**, 74, 3.
- (23) Tan, P. H.; Dimovski, S.; Y., G. *Philos. Trans. R. Soc. London, Ser. A* **2004**, 362, 2289–2310.
- (24) Reich, S.; Thomsen, C. *Philos. Trans. R. Soc. London, Ser. A* **2004**, 362 (1824), 2271–2288.
- (25) Mykhaylyk, O. O.; Solonin, Y. M.; Batchelder, D. N.; Brydson, R. *J. Appl. Phys.* **2005**, 97, 7.
- (26) Aleksenskii, A. E.; Osipov, V. Y.; Vul, A. Y.; Ber, B. Y.; Smirnov, A. B.; Melekhin, V. G.; Adriaenssens, G. J.; Iakubovskii, K. *Phys. Solid State* **2001**, 43 (1), 145–150.

- (27) Ferraro, J. R.; Nakamoto, K., *Introductory Raman Spectroscopy*; Academic Press: New York, 2003; pp 118–128.
- (28) Casiraghi, C.; Piazza, F.; Ferrari, A. C.; Grambole, D.; Robertson, J. *Diamond Relat. Mater.* **2005**, 14, 1098–1102.
- (29) Yushin, G. N.; Osswald, S.; Padalko, V. I.; Bogatyreva, G. P.; Gogotsi, Y. *Diamond Relat. Mater.* **2005**, 14 (10), 1721–1729.

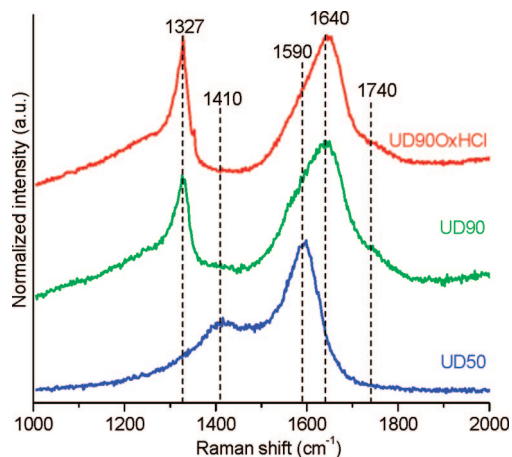


Figure 1. Room-temperature UV Raman spectra of nanodiamond powders.

and C=O and O–H containing surface functional groups as revealed by IR spectroscopy. UD90OxHCl is a product of UD90Ox treatment with boiling aqueous HCl to remove metallic impurities, which become accessible after air oxidation. UD90H was produced by heating UD90 in a H₂ atmosphere at 800 °C for 2 h.³⁰

UV Raman spectra were recorded using a Renishaw 1000/2000 spectrometer with a HeCd laser (λ_{exc} 325 nm) in a backscattering geometry. In a series of experiments (when indicated), water was used to eliminate laser-induced heating. No cooling agents were used elsewhere; instead the incident laser power was minimized to 0.4 mW (15 \times objective).

UV Raman spectra of UD90 powders at elevated temperatures were recorded in steady Ar flow using a controlled environment temperature-programmed hot stage with a quartz window (Linkam).

Results and Discussion

The UV Raman spectra of three ND powders are shown in Figure 1. UD50 exhibits the characteristic Raman features of graphitic carbon: the G-band at 1590 cm⁻¹ and the disorder-induced D-band at \sim 1400 cm⁻¹. The Raman signal of diamond cannot be observed because the diamond core is shielded by surrounding graphitic layers and amorphous carbon.⁶ The Raman spectra of UD90 and UD90OxHCl are similar to each other and are both noticeably different from UD50. They show an asymmetrically broadened sharp diamond peak at 1327 ± 2 cm⁻¹ with a shoulder toward lower wavenumbers, and a broad, asymmetric peak with a maximum at 1640 cm⁻¹. Thus, there is no general “Raman spectrum of ND”, as it varies for different ND grades. Furthermore, while the peak at 1590 cm⁻¹ in UD50 can be identified as G-band of graphitic carbon, the assignment of the peak at 1640 cm⁻¹ observed in UD90 and UD90OxHCl as well as in many other ND samples reported in the literature^{20,25,31,32} is not straightforward.

To further investigate the origin of the 1640 cm⁻¹ peak, we monitored temperature-induced changes in the Raman

spectrum of ND. In situ Raman spectra were recorded in Ar flow to avoid sample oxidation, changes of the surface chemistry and adsorption from air. As expected for the G-band in graphitic materials, the 1640 cm⁻¹ peak showed a red shift with an increase in temperature (Figure 2a). However, the slope of the curve was much steeper than for graphite or nanotubes,^{33,34} the temperature dependence was nonlinear, and the shape of the 1640 cm⁻¹ ND peak changed upon heating. Subsequent cooling of the sample down to room temperature in Ar flow did not restore the original shape (Figure 2a) or position (Figure 3) of the peak. Although the intensity of the peak is nearly constant during the heating–cooling cycle, the peak asymmetry decreases at higher temperatures and disappears around 200 °C. The peak asymmetry does not reappear upon cooling down to room temperature in Ar flow (Figure 2a), but is restored after a few minutes of exposing the cooled sample to ambient air (Figure 2b) by opening the heating stage. These changes are not what one would expect for a temperature-induced shift of the G-band. The thermal shift of the G-band in graphitic materials is known to be completely reversible and a linear function of temperature between 25 and 500 °C.^{33,34} Using the same experimental conditions, we measured the temperature changes of the G-band of vacuum-annealed UD50 composed of onion-like graphitic particles with sizes of 5–50 nm³⁰ (inset in Figure 3). As expected, the position of the G-band for this material was found to be fully reversible and a linear function of temperature with a derivative of 0.029 cm⁻¹/°C, which is close to that of carbon nanotubes (0.023 – 0.030 cm⁻¹/°C).^{33,34} It is interesting that while very different from the temperature shift of the G-band of carbon onions during heating, the 1640 cm⁻¹ peak shift of UD90 upon cooling was close to the temperature behavior of the G-band of the onions (Figure 3).

This unusual temperature behavior contradicts several assignments of the 1640 cm⁻¹ peak in the Raman spectrum of ND proposed in literature suggesting that it cannot originate from: surface sp² carbon,^{21,31} surface amorphous carbon,³² mixed sp²/sp³ carbon,²⁵ or split interstitial defects inside the diamond core of ND,²⁰ as they should all result in small, linear and reversible changes within the temperature range 25–300 °C. Although it was shown before that split interstitial defects in bulk diamond can be “healed” by annealing in an inert atmosphere,³⁵ it happens at temperatures much higher than 300 °C. Moreover, once the defects have been annealed, they could not be restored simply by exposing the cooled sample to air, as observed in the case of the 1640 cm⁻¹ peak in the Raman spectrum of ND (Figure 2b).

Taking into account the observed heating–cooling behavior, we put forward a different explanation regarding the origin of the 1640 cm⁻¹ peak in ND. The irreversible loss of asymmetry during heating–cooling in an inert gas flow could be accounted for by the removal of some surface species which contribute to the Raman spectrum of ND and

(30) Mochalin, V. N.; Osswald, S.; Portet, C.; Yushin, G.; Hobson, C.; Havel, M.; Gogotsi, Y. *Mater. Res. Soc. Symp. Proc.* **2008**, 1039, 1039–P11–03.

(31) Aleksenskii, A. E.; Osipov, V. Y.; Vul', A. Y.; Ber, B. Y.; Smirnov, A. B.; Melekhin, V. G.; Adriaenssens, G. J.; Yakubovskii, K. *Phys. Solid State* **2001**, 43 (1), 145–150.

(32) Khasawinah, S. A.; Popovici, G.; Farmer, J.; Sung, T.; Prelas, M. A.; Chamberlain, J.; White, H. J. *Mater. Res.* **1995**, 10 (10), 2523–2530.

(33) Osswald, S.; Flahaut, E.; Gogotsi, Y. *Chem. Mater.* **2006**, 18 (6), 1525–1533.

(34) Osswald, S.; Havel, M.; Gogotsi, Y. *J. Raman Spectrosc.* **2007**, 38 (6), 728–736.

(35) Kalish, R.; Reznik, A.; Praver, S.; Saada, D.; Adler, J. *Phys. Status Solidi A* **1999**, 174 (1), 83–99.

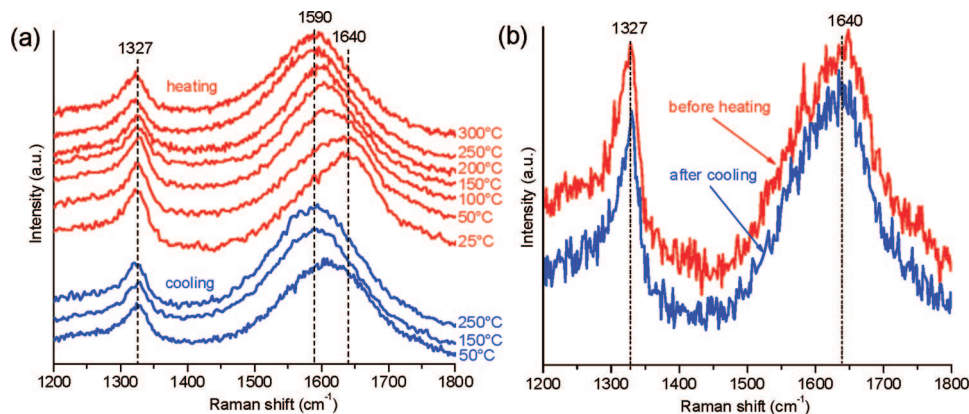


Figure 2. (a) UV Raman spectra of NDALit in Ar atmosphere at different temperatures and (b) UV Raman spectra of NDALit recorded in air at room temperature before heating and after cooling.

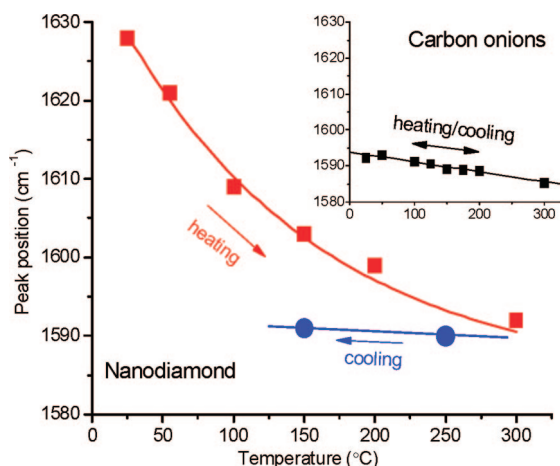


Figure 3. Temperature dependence of the 1640 cm^{-1} Raman peak position of NDALit in comparison to G-band of carbon onions. Arrows indicate temperature changes.

to the observed peak asymmetry. The subsequent restoration of the asymmetric peak shape upon exposure to ambient air implies that those species are recreated on the surface of ND, which can be explained by adsorption of or reaction with components of air. The two likeliest bond vibrations that give rise to Raman peaks in this range are O–H bending and C=O stretching.³⁶ To distinguish between these two contributions, we eliminated C=O containing groups from the surface of ND by annealing the UD90 powder in hydrogen.³⁰ The contribution of carbonyl groups is ruled out by observation of the Raman peak at 1640 cm^{-1} for the hydrogenated sample (Figure 4a), which shows no traces of C=O in FTIR (Figure 4b).

At the same time, O–H peaks in FTIR are not influenced by the hydrogen annealing, supporting the hypothesis that O–H bending vibrations can contribute to the 1640 cm^{-1} peak. Selective removal of O–H containing groups from the surface of ND would provide a direct test of this hypothesis. Unfortunately, it is difficult to realize without simultaneously changing the sp^2/sp^3 carbon ratio. Hydrogen treatment does not remove hydroxyl groups. Moreover, depending on conditions of the treatment, it can increase the O–H content as a result of C=O to C–O–H conversion.³⁰ High-

temperature inert gas annealing, which removes all functional groups,³⁰ cannot be used because it leads to the graphitization of ND, which will naturally affect the shape and position of the 1640 cm^{-1} Raman peak.

On the basis of the presented analysis, we thus assume that the 1640 cm^{-1} peak in the Raman spectrum of ND results from overlapping of contributions from sp^2 carbon and O–H bending vibrations. The source of O–H vibrations is either covalently attached surface functional groups and/or adsorbed water. ND powders readily adsorb moisture from air, surpassing many other carbon nanomaterials in this respect, as illustrated by the TGA curves recorded in air (Figure 5). The initial weight loss of 7–10% on a UD90 curve at temperature below the onset of carbon oxidation at $350\text{--}400\text{ }^\circ\text{C}$ ⁶ corresponds mainly to water desorption.

To monitor the removal of O–H-containing species and related changes in the 1640 cm^{-1} peak, we recorded FTIR spectra of UD90 at elevated temperatures (Figure 6). As the quartz window of the heating stage absorbs in IR, it was impossible to record the FTIR spectra in Ar atmosphere; therefore, the spectra in Figure 6 were recorded in air. Upon heating, the IR peak at 1640 cm^{-1} underwent a slight red shift between 100 and $300\text{ }^\circ\text{C}$. The shift may be induced by the weakening of O–H bonds with temperature or by the gradual removal of O–H groups (both of chemically linked and adsorbed species), revealing a peak of conjugated C=C stretch vibrations located at $1600\text{--}1620\text{ cm}^{-1}$.³⁶ The O–H stretch band (a broad peak at $3200\text{--}3600\text{ cm}^{-1}$ in Figure 6) is significantly decreased at $T \geq 200\text{ }^\circ\text{C}$ suggesting that at $T \geq 200\text{ }^\circ\text{C}$ the stretching of conjugated C=C bonds is the main reason for the $\sim 1620\text{ cm}^{-1}$ IR absorption. At $425\text{ }^\circ\text{C}$, the oxidation of sp^2 carbon in ND powders⁶ leads to the disappearance of the small broad C=C peak at $\sim 1600\text{ cm}^{-1}$ within 60 min (Figure 6). When the sample is cooled down to room temperature after being held for 2 h at $425\text{ }^\circ\text{C}$ in air, the peak at 1640 cm^{-1} is restored (Figure 6), suggesting a significant contribution from O–H bending vibrations at room temperature. The observed temperature trend of the 1640 cm^{-1} IR peak of UD90 is in good agreement with previous results.³⁷ However, it should be noted that the temperature at which this IR peak begins to change or completely disappears depends on the surface chemistry of ND and can vary for different powders. For example, in the

(36) Speight, J. G. *Lange's Handbook of Chemistry*, 16th ed.; McGraw-Hill: New York, 2005; p 1572.

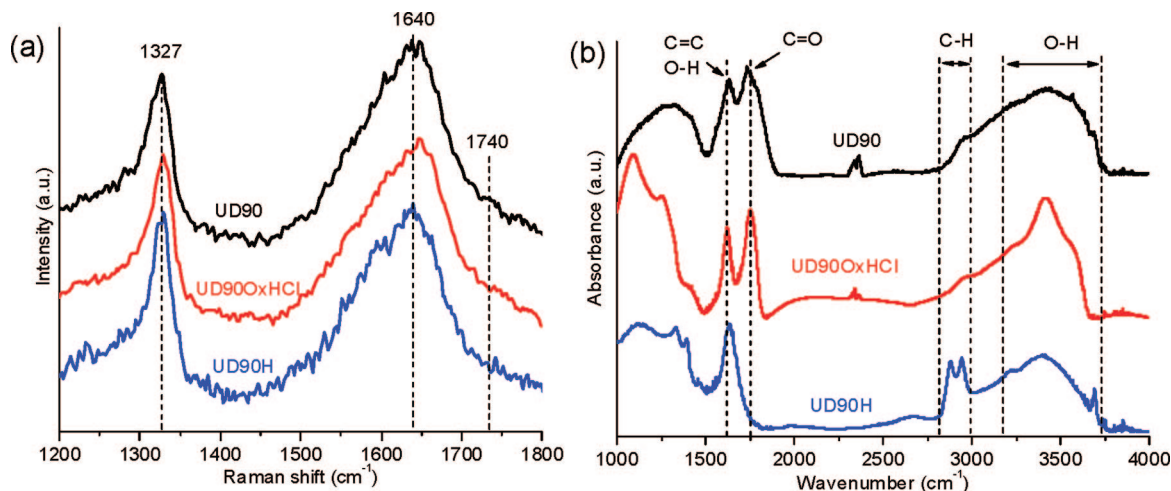


Figure 4. (a) UV Raman and (b) FTIR spectra of nanodiamond powders with different surface chemistry.

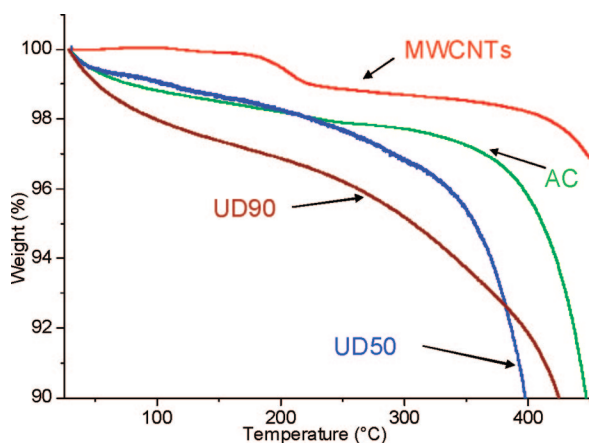


Figure 5. TGA curves of different carbon materials recorded in air at 1 °C/min heating rate.

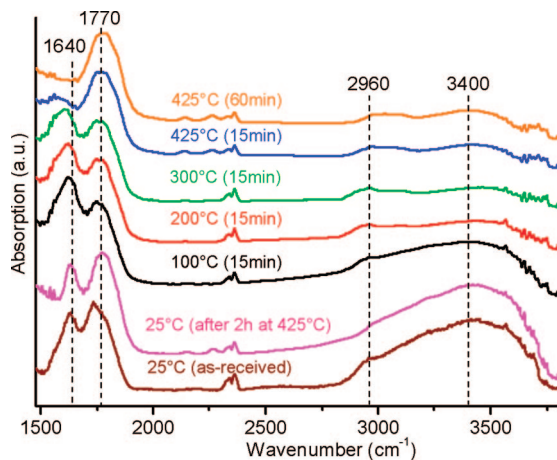


Figure 6. In situ FTIR spectra of UD90 held at specified temperatures and cooled to room temperature after being held for 2 h at 425 °C. All spectra were recorded from nanodiamond being in contact with air all time.

case of NDAlit powder (not shown), we have found that the IR peak at 1620–1640 cm⁻¹ totally disappears within 5 min at 300 °C in air.

Several other experiments were carried out in order to test the O–H contribution hypothesis. UV Raman spectra of UD90Ox recorded at room temperature and normalized with respect to the intensity of the 1640 cm⁻¹ peak are shown in

Figure 7. Oxidation in air results in the removal of sp² carbon and formation of oxygen containing surface functional groups such as O–H, COOH, C=O, (CO)₂O (anhydro-), etc.⁶ If the entire 1640 cm⁻¹ peak were a peak of sp² carbon, then a longer oxidation time would simply result in a decrease of the intensity of this peak. It turns out that not only the intensity but also the shape of this peak is changed with oxidation time (Figure 7). Both changes are natural under the assumption that the 1640 cm⁻¹ peak is a superposition of the G-band of graphitic carbon and O–H bending vibrations from either adsorbed or covalently linked species on the surface of ND. With longer oxidation time, the relative intensity of the G-band (at 1590 cm⁻¹) decreases compared to the O–H bending (at 1640 cm⁻¹) (Figure 7a). Peak fitting using three Lorentz functions fixed at 1590, 1640, and 1740 cm⁻¹ reproduces the overall shape of the composite peak and the trend of the sp²/O–H ratio with increasing oxidation time (Figure 7b). The peak fitting also gives an idea of the overestimation that is potentially introduced when evaluating the amount of nondiamond carbon content based on the Raman spectra, assuming the whole 1640 cm⁻¹ peak to be a peak of sp² carbon. Oxidation, which increases the content of carbonyl groups, also results in a pronounced shoulder at ~1740 cm⁻¹ (Figure 7a), which is the correct position for the C=O stretching Raman peak.³⁶ Thus, the spectra in Figure 7 show that the 1640 cm⁻¹ peak is a superposition of the G-band of graphitic carbon, the O–H bending and C=O stretching vibrations.

Annealing of UD90Ox in Ar at 700–900 °C leads to the opposite trend in the O–H/sp² peak ratio (Figure 8), which corresponds to the progressive removal of O–H groups and an increase in sp² carbon content with annealing temperature. At higher temperatures, the Ar annealing would completely remove surface functionalities and convert ND particles into carbon onions³⁰ with the 1640 cm⁻¹ Raman peak being transformed into the G-band of graphitic carbon positioned at 1590 cm⁻¹.

A very important consequence of the O–H contribution to the Raman spectrum of ND is related to the use of liquid water as a cooling medium recommended for minimizing laser-induced thermal damage of a sample in UV Raman spectroscopy. The recommendation to use water is based on

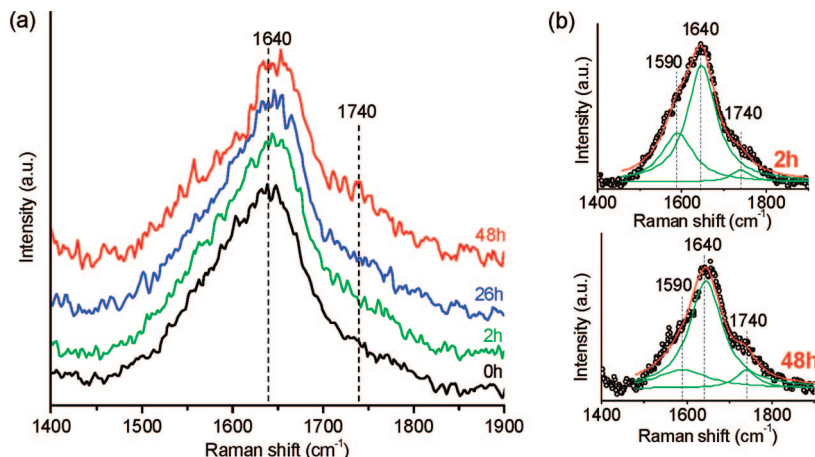


Figure 7. (a) UV Raman spectra of as-received and air-oxidized UD90 and (b) examples of peak fitting for samples oxidized for 2 and 48 h with three Lorentz functions fixed at 1590, 1640, and 1740 cm^{-1} .

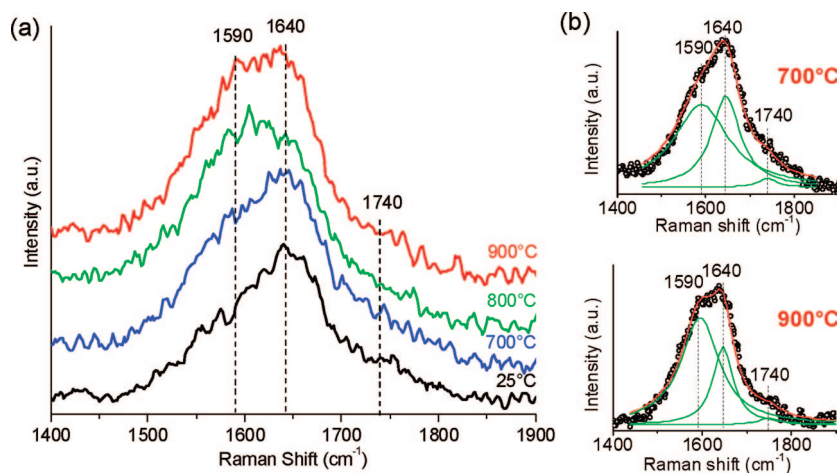


Figure 8. (a) UV Raman spectra of air-oxidized UD90 before and after Ar annealing for 1 h at specified temperature and (b) examples of peak fitting for samples annealed at 700 and 900 $^{\circ}\text{C}$ with three Lorentz functions fixed at 1590, 1640, and 1740 cm^{-1} .

the assumption that it does not interfere with Raman spectra. Indeed, a low sensitivity of Raman spectroscopy toward water is a well-known advantage over IR spectroscopy (see for example p 119 in ref 27), and is often mentioned as a reason for a wide use of Raman spectroscopy in studying biomolecules in physiological aqueous environments. However, if the Raman signal of a material is weak, as in the case of ND, then even a small contribution from water cannot be neglected. This contribution has recently been mentioned for Raman spectra of aqueous suspensions of carbon nanotubes,³⁸ where the G-band was much stronger than for a typical ND powder. In our experiments, we observed that for UD90 recorded under a layer of water in a Petri dish, the intensity of the 1640 cm^{-1} Raman peak noticeably increased, even when the thickness of the water layer was just a fraction of a millimeter (Figure 9).

If the thickness was a millimeter or more, the intensity of this peak increased dramatically. In previously published studies, when water cooling was used for ND, there were no indications of control over the water layer thickness. As

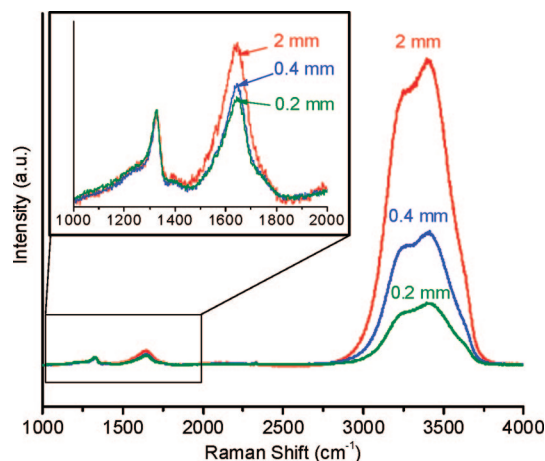


Figure 9. Contribution of water coolant to the 1640 cm^{-1} peak in the Raman spectra of ND powder recorded through different thicknesses (in mm) of the water layer.

such, the 1640 cm^{-1} peak measured with this technique may turn out to be mainly attributed to O–H bending vibrations in liquid H_2O . In addition, water has a strong stretching O–H Raman mode at 3300–3700 cm^{-1} , broadened because of hydrogen bonds (Figure 10).

However, in contrast to the 1640 cm^{-1} O–H peak, which requires careful analysis in order to be detected, the water-

(37) Ji, S. F.; Jiang, T. L.; Xu, K.; Li, S. B. *Appl. Surf. Sci.* **1998**, 133 (4), 231–238.

(38) Salzmann, C. G.; Chu, B. T. T.; Tobias, G.; Llewellyn, S. A.; Green, M. L. H. *Carbon* **2007**, 45 (5), 907–912.

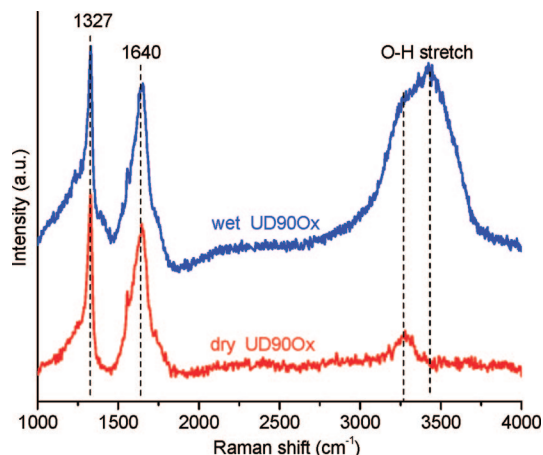


Figure 10. Contribution of water coolant to first- and second-order UV Raman spectrum of ND powder.

related O–H stretch band is so intense that it totally overwhelms the C–H range and the second-order Raman spectrum of carbon and can thus be easily detected even at very low water concentration, when no liquid water is apparently present, as shown in Figure 10.

Therefore, it is extremely important to analyze possible contributions from coolants such as water, especially when deriving any conclusions based on the peaks between 1500 and 1800 cm^{-1} , such as the D/G intensity ratio commonly used for evaluating ordering in carbon materials, or $\text{sp}^2/\text{diamond}$ carbon ratio for ND. In such cases, for the purpose of cooling, other liquids may be considered having no peaks in the range of interest (for instance, high purity CCl_4 or CS_2 , which show peaks only below 1000 cm^{-1} in Raman spectra,²⁷ though both should be used with great precautions as they are toxic). In any event, possible coolant interference must be examined and properly accounted for.

Assuming the hypothesis of strong O–H bending contribution to the Raman spectrum of ND is true, an unusually low intensity of Raman signal in the range 3000–3700 cm^{-1} as compared to the peak at 1640 cm^{-1} for a dry UD90Ox sample (Figure 10) should be mentioned. The 3000–3700 cm^{-1} range corresponds to O–H stretching vibrations, which are typically more intense than O–H bending vibrations. Indeed, the difference can clearly be seen by comparing the intensities of 1640 cm^{-1} and 3000–3700 cm^{-1} peaks in a spectrum of bulk water (Figure 9). However, for water molecules confined in a small volume on the surface or between the aggregated ND particles, the ratio of the intensities can be significantly different from that observed in bulk water. It has been theoretically shown before for water inside single-walled carbon nanotubes that the confinement reduces the number of hydrogen bonds from 2–4 per H_2O molecule in bulk water to just 1.³⁹ Reduction in hydrogen bond number results in splitting the broad O–H stretch peak into 2 peaks: one located between 3000 and 3500 cm^{-1} corresponds to O–H groups involved in hydrogen bonding between H_2O molecules and has intensity lower than the of O–H; and the other, narrower, corresponding to non-hydrogen bonded O–H groups, located at higher frequency

and having higher intensity. Because the non-hydrogen bonded O–H groups of water in a nanotube are subjected to steric hindrance regarding the stretching vibrations, the position of the second O–H stretch peak is predicted to be unusually high ($>4000 \text{ cm}^{-1}$).³⁹ For a dry UD90Ox sample (Figure 10) we observed a small broad peak at 3270 cm^{-1} and no other peaks up to 4000 cm^{-1} (the upper limit of the Raman shift scale for our spectrometer). Thus, the unusual intensity ratio of O–H bending and stretching vibrations, observed for a dry UD90Ox powder in Figure 10, can be attributed to the effect of confinement of O–H stretching vibrations, which is currently studied theoretically for carbon nanotubes^{39,40} and other porous materials, and may take place in confined space between the particles in dry nanodiamond powder. Water confinement in nanodiamond powders clearly should be studied further and to support the explanation above, we just want to mention that nanophase of water around nanodiamond particles has been recently found in nanodiamond gels by DSC⁴¹ and its unusual thermodynamic properties were well-explained by the confinement.

Conclusions

A critical discussion of the 1640 cm^{-1} peak observed in UV Raman spectra of ND powders based on extensive Raman and FTIR studies has been presented. It has been shown that this peak cannot be assigned solely to surface graphitic carbon, amorphous carbon, mixed sp^2/sp^3 carbon or split interstitial (dumb-bell) defects inside the diamond core of ND. In particular, none of these factors can explain the observed changes in the position and shape of this peak during a heating–cooling cycle in an inert atmosphere and subsequent exposure of the sample to ambient air. Oxidation, hydrogenation and annealing in an inert atmosphere allowed us to discriminate between C=O and O–H contributions to this peak. All experimental observations are easily explained if the broad asymmetric 1640 cm^{-1} Raman peak of ND is assigned to a superposition of sp^2 carbon band at 1590 cm^{-1} with a peak of O–H bending vibrations at 1640 cm^{-1} . C=O stretching vibrations, which are shown to be positioned at 1740 cm^{-1} in the Raman spectrum of oxidized ND, produce a shoulder on the 1640 cm^{-1} peak. This assignment of the 1640 cm^{-1} Raman peak emphasizes the importance of correctly accounting for the O–H contribution in Raman spectra of ND and other carbon nanomaterials, especially when water cooling of the sample is used.

Acknowledgment. The authors thank NanoBlox, Inc., for providing samples of nanodiamond powders for this work. Financial support was provided through an NTI grant by Ben Franklin Technology Partners of Southeastern Pennsylvania. The authors also acknowledge Dr. Z. Nikolov and the Centralized Research Facilities (CRF) of the College of Engineering for providing access to the equipment used for this research. Elizabeth Dreher read the manuscript and helped to improve its quality. V. Mochalin appreciates a stimulating discussion with Prof. Stephen Prawer from Melbourne University.

CM802057Q

(40) Marti, J.; Gordillo, M. C. *Phys. Rev. B* **2001**, *63*, 16.

(41) Korobov, M. V.; Avramenko, N. V.; Bogachev, A. G.; Rozhkova, N. N.; Osawa, E. *J. Phys. Chem. C* **2007**, *111* (20), 7330–7334.

(39) Mann, D. J.; Halls, M. D. *Phys. Rev. Lett.* **2003**, *90*, 19.